EVOLUTION AND STABILITY OF THE G-MATRIX ON A LANDSCAPE WITH A MOVING OPTIMUM

Author(s): Adam G. Jones, Stevan J. Arnold, Reinhard Burger
Source: Evolution, 58(8):1639-1654.
Published By: The Society for the Study of Evolution
https://doi.org/10.1554/03-651
URL: http://www.bioone.org/doi/full/10.1554/03-651

EVOLUTION

INTERNATIONAL JOURNAL OF ORGANIC EVOLUTION

PUBLISHED BY

THE SOCIETY FOR THE STUDY OF EVOLUTION

Vol. 58 **August 2004** **No. 8**

Evolution, 58(8), 2004, pp. 1639–1654

EVOLUTION AND STABILITY OF THE **G**-MATRIX ON A LANDSCAPE WITH A MOVING OPTIMUM

ADAM G. JONES,[1,2] STEVAN J. ARNOLD,[3] AND REINHARD BÜRGER[4]

[1]*School of Biology, Georgia Institute of Technology, 310 Ferst Drive, Atlanta, Georgia 30332*

[2]*E-mail: adam.jones@biology.gatech.edu*

[3]*Department of Zoology, 3029 Cordley Hall, Oregon State University, Corvallis, Oregon 97331*

[4]*Institut für Mathematik, Universität Wien, Strudlhofgasse 4, 1090 Wien, Austria*

Abstract.—In quantitative genetics, the genetic architecture of traits, described in terms of variances and covariances, plays a major role in determining the trajectory of evolutionary change. Hence, the genetic variance-covariance matrix (**G**-matrix) is a critical component of modern quantitative genetics theory. Considerable debate has surrounded the issue of **G**-matrix constancy because unstable **G**-matrices provide major difficulties for evolutionary inference. Empirical studies and analytical theory have not resolved the debate. Here we present the results of stochastic models of **G**-matrix evolution in a population responding to an adaptive landscape with an optimum that moves at a constant rate. This study builds on the previous results of stochastic simulations of **G**-matrix stability under stabilizing selection arising from a stationary optimum. The addition of a moving optimum leads to several important new insights. First, evolution along genetic lines of least resistance increases stability of the orientation of the **G**-matrix relative to stabilizing selection alone. Evolution across genetic lines of least resistance decreases **G**-matrix stability. Second, evolution in response to a continuously changing optimum can produce persistent maladaptation for a correlated trait, even if its optimum does not change. Third, the retrospective analysis of selection performs very well when the mean **G**-matrix ($\bar{\mathbf{G}}$) is known with certainty, indicating that covariance between **G** and the directional selection gradient $\boldsymbol{\beta}$ is usually small enough in magnitude that it introduces only a small bias in estimates of the net selection gradient. Our results also show, however, that the contemporary **G**-matrix only serves as a rough guide to $\bar{\mathbf{G}}$. The most promising approach for the estimation of $\bar{\mathbf{G}}$ is probably through comparative phylogenetic analysis. Overall, our results show that directional selection actually can increase stability of the **G**-matrix and that retrospective analysis of selection is inherently feasible. One major remaining challenge is to gain a sufficient understanding of the **G**-matrix to allow the confident estimation of $\bar{\mathbf{G}}$.

Key words.—Adaptive landscape, genetic correlation, genetic covariance, genetic variance, net selection gradient, pleiotropy, response to selection, quantitative genetics.

Received November 10, 2003. Accepted May 4, 2004.

The **G**-matrix plays a central role in quantitative theory for the evolution of continuously distributed traits that are affected by many genes. This matrix (with additive genetic variances on its main diagonal and additive genetic covariances elsewhere) describes the dispersion of genetic values within populations. The **G**-matrix profoundly affects the population's ability to respond to selection and its vulnerability to genetic drift (Lande 1979). It can be used to assess the population's capacity to evolve in response to selection, reconstruct historical patterns of selection, and test genetic drift as a null model for differentiation. In all of these contexts, stability of the **G**-matrix is an important but unresolved problem. Because the **G**-matrix is bound to fluctuate in a population of finite size (Lande 1979), the question of stability does not have a simple yes or no answer. Instead we must consider a set of more subtle issues. What types of quantitative characters have relatively stable **G**-matrices and over what time scale? How much are evolutionary inferences affected by systematic and random changes in the **G**-matrix?

Slow progress toward a resolution of the issue of **G**-matrix stability is primarily a result of theoretical limitations. The theoretical characterization of the **G**-matrix after it has equilibrated under a static regime of selection, mutation, and recombination has only been achieved under various sets of simplifying assumptions, beyond assumptions of additivity, linkage equilibrium, and infinite population size. Analytical approximations for the magnitude of the constituent variances and covariances at mutation-selection balance have been obtained by assuming a multivariate Gaussian distribution of allelic effects (Lande 1980a); assuming that mutational effects are much larger than the standing genetic variation, leading to a pleiotropic house-of-cards approximation (Tur-

elli 1985); and assuming a certain model of constrained pleiotropic effects (Wagner 1989). For finite populations, no theoretical predictions for the multivariate case have yet been derived. In addition, we do not have equations for the generation-by-generation dynamics of the evolving **G**-matrix, except under very special assumptions, such as Bulmer's infinitesimal model (Turelli 1985). Even in the case of a single character, these issues are fairly complex, and it has been shown that the dynamics of the genetic variance depends on the higher moments of the distribution of allelic effects as well as on other genetic details (Turelli and Barton 1990; Bürger 2000). Consequently, we cannot predict how much the **G**-matrix will wobble and fluctuate due to the interaction of genetic drift with selection, mutation, and recombination, even if the adaptive landscape remains constant. For all these reasons, the stability of the **G**-matrix has been viewed as an empirical issue (Turelli 1988; Steppan et al. 2002).

The empirical investigation of **G**-matrix stability is also plagued by limitations. The empirical studies have been by comparison of matrices sampled from nature or from experimental lines. A strength of comparing matrices from natural populations is that the results are likely to reflect responses under natural conditions. The histories of selection and population size may be unknown, but at least they are representative of the real world. A limitation in nonexperimental work is that usually only two or three matrices are available for comparison, because of the difficulty of assembling the large samples of families needed to estimate **G**. Nevertheless, comparative work of this kind has revealed some intriguing results. Although **G**-matrices can differ appreciably, especially among distantly related species or populations (Kohn and Atchley 1988; Paulsen 1996), they often show conserved aspects of structure (Arnold 1981; Arnold and Phillips 1999; Roff and Mousseau 1999). In particular, the eigenvectors (principal components) of the matrix often are conserved even though eigenvalues vary. What accounts for this conservation? On the experimental side, **G**-matrices have been compared after separate lines have been exposed to deliberate directional selection or allowed to drift. A strength of this approach is that selection is imposed and population size is known. A limitation is that stabilizing, stability-conferring aspects of selection may be missing and the force of directional selection may be far stronger than is typical in nature. Given these probable departures from selection regimes in nature, the result that experimental lines sometimes show similar **G**-matrices is particularly surprising (Wilkinson et al. 1990; Shaw et al. 1995). Experiments have also established that the **G**-matrix can wobble, that is, inflate and contract in the absence of selection, especially in small populations (Phillips et al. 2001). While computer simulations of evolving **G**-matrices do not solve all of the problems that plague empirical comparisons, they do offer a complementary approach to the problem of **G**-matrix stability.

The goal of this article is to extend past simulation work on the evolution of the **G**-matrix. Several studies have used a simulation-based approach to study various aspects of multivariate quantitative trait evolution (Wagner 1989; Baatz and Wagner 1997; Wagner et al. 1997; Reeve 2000; Jones et al. 2003), but only one has focused specifically on **G**-matrix stability (Jones et al. 2003). In that study, we examined the evolution and stability of the **G**-matrix in response to a stabilizing adaptive landscape that is constant in configuration and position (Jones et al. 2003). We chose a stabilizing landscape because this form of selection is often found in empirical studies (Lynch 1989; Kingsolver et al. 2001) and is the mode of selection that best accounts for conservatism in morphology and long-term stasis in phenotypic traits (Simpson 1944; Schmalhausen 1949; Charlesworth et al. 1982). One of our main findings was that different aspects of stability react differently to selection, mutation, and drift. In particular, we found that correlational selection, pleiotropic mutation, and large population size promoted stability of the orientation of the **G**-matrix. In contrast, stability in the overall size and shape of the **G**-matrix was increased only by population size. In the present study we allow the adaptive peak to move while the landscape itself maintains a constant configuration. This model of selection may correspond to temporal change in the environment or the invasion of a new adaptive zone (Simpson 1944, 1953). The present explorations are limited, however, to movement of the peak at a constant speed. The main question that concerns us is how different aspects of **G**-matrix stability respond to the speed and direction of peak movement. A secondary goal is to determine the degree to which stochastic variation in the **G**-matrix affects evolutionary inferences.

Stochastic variation in **G** carries important implications for evolutionary inference, because of the central role that the **G**-matrix plays in equations for evolutionary change. If fluctuations in **G** were relatively minor, one could ignore variation in **G** and use an estimate of average **G** to make evolutionary inferences. In this spirit, a single value or an average value of **G** has been used to make predictions about genetic drift, predict potential responses to selection, or reconstruct historical patterns of directional selection (Lande 1979; Price and Grant 1985; Cheverud 1996). Reconstructions of historical selection have relied on Lande's (1979) expression for the net directional selection gradient, but fluctuation and evolution of the **G**-matrix might add considerable barriers to success in this endeavor (Turelli 1988; Shaw et al. 1995). We assess the impact of systematic and stochastic variation in the **G**-matrix on the estimation of the net directional selection gradient. This assessment will take us one more step toward understanding whether instability of **G** is likely to have important effects on this and other kinds of evolutionary inference.

Theoretical Background

Some theoretical results will be useful in understanding our simulations and interpreting our results. We consider two phenotypic characters that evolve in response to a Gaussian adaptive landscape with a moving optimum. The population mates randomly and has discrete generations. Viability selection is imposed by a Gaussian individual selection surface such that the fitness of individuals with phenotype $\mathbf{z}$ is given by

$$W(\mathbf{z}) \propto \exp[(\mathbf{z} - \boldsymbol{\theta})^{\mathrm{T}}\boldsymbol{\omega}^{-1}(\mathbf{z} - \boldsymbol{\theta})], \qquad (1)$$

where $\mathbf{z}$ is the column vector of trait values, $\boldsymbol{\omega}$ is the matrix of coefficients that describe the strengths of stabilizing and correlational selection, $\boldsymbol{\theta}$ is the position of the optimum, and

T denotes transposition. We assume that the optimum $\boldsymbol{\theta} = \boldsymbol{\theta}_t$, where the subscript t indicates the generation, changes at a constant rate and in a given (constant) direction $\boldsymbol{\Delta\theta} = (\Delta\theta_1, \Delta\theta_2)^{\mathrm{T}}$ that is, $\boldsymbol{\theta}_{t+1} - \boldsymbol{\theta}_t \equiv \boldsymbol{\Delta\theta}$.

We denote the distribution of phenotypes by $p(\mathbf{z})$, its mean by $\bar{\mathbf{z}}$, and its variance-covariance matrix before selection by $\mathbf{P}$. In this, and only this, section, we assume that $p(\mathbf{z})$ is multivariate normal. Following the classical additive model of quantitative genetics, we assume that $\mathbf{P} = \mathbf{G} + \mathbf{E}$, where $\mathbf{G}$ is the genetic covariance matrix (the **G**-matrix for short), $\mathbf{E}$ is the covariance matrix of environmental effects (which, by an appropriate linear transformation, may be assumed to have entries 1 on its diagonal and 0 elsewhere). Because genotype-environment interaction is ignored, the mean phenotypic vector $\bar{\mathbf{z}}$ equals the vector of mean breeding (genotypic) values.

Mean fitness in the population is given by the (multivariate) integral $\bar{W} = \int W(\mathbf{z})p(\mathbf{z})d\mathbf{z}$. Corresponding to the individual selection surface $W(\mathbf{z})$, there is an adaptive landscape that affects the evolution of the phenotypic mean $\bar{\mathbf{z}}$ and, in general, the whole population distribution. This landscape describes $\bar{W}$ as a function of $\bar{\mathbf{z}}$. Because $p(\mathbf{z})$ is Gaussian, the population's fitness landscape $\bar{W}$ is again Gaussian with optimum $\boldsymbol{\theta}$ and with shape parameters given by the matrix $\boldsymbol{\omega} + \mathbf{P}$ (Lande 1979). The force of the directional selection on the traits can be described by the directional selection gradient,

$$\boldsymbol{\beta} = \nabla \ln \bar{W} = \left(\frac{\partial \ln \bar{W}}{\partial \bar{z}_1}, \frac{\partial \ln \bar{W}}{\partial \bar{z}_2} \right)^{\mathrm{T}}, \tag{2}$$

where ∇ denotes the gradient operator of partial derivatives with respect to the single-trait means (Lande 1979). The deterministic response of the mean $\bar{\mathbf{z}}$ to selection is not in the direction of steepest uphill slope, which is given by $\boldsymbol{\beta}$. Instead the population mean evolves in a direction given by

$$\Delta\bar{\mathbf{z}} = \mathbf{G}\boldsymbol{\beta} \tag{3}$$

(Lande 1979). It is important to note that equation (3) is only an approximation because it assumes multivariate normality of the phenotypic distribution. For a discussion of the much better understood univariate case see Bürger (2000, pp. 193–197). However, equation (3) does not require that $\mathbf{G}$ or $\boldsymbol{\beta}$ are constant in time.

A population evolving in response to a moving adaptive landscape will experience directional selection and lag behind the moving peak (Lynch et al. 1991). In the case of a population reacting to a moving Gaussian adaptive landscape that has a constant shape, the force of directional selection in any given generation t is proportional to the deviation of the phenotypic mean from the peak of the landscape,

$$\boldsymbol{\beta}_t = (\boldsymbol{\omega} + \mathbf{P}_t)^{-1}(\boldsymbol{\theta}_t - \bar{\mathbf{z}}_t), \tag{4}$$

where $\mathbf{P}_t$ is the phenotypic variance-covariance matrix before selection in generation t (Lande 1980b). An evolving population may lag substantially behind and away from the moving optimum. In the case of an infinitely large population that has equilibrated with the moving peak, that is, in the absence of stochastic fluctuations, the expected lag is given by the vector

$$\mathbf{L} = \boldsymbol{\theta}_t - \bar{\mathbf{z}}_t = (\boldsymbol{\omega} + \mathbf{P})\mathbf{G}^{-1}\boldsymbol{\Delta\theta} \tag{5}$$

(for t sufficiently large), where $\boldsymbol{\Delta\theta}$ is the per generation change in the position of the optimum. This expression generalizes the univariate approximation of Lynch and Lande (1993). Such a population will lag directly behind the moving optimum when $\mathbf{G}$ is proportional to $\boldsymbol{\omega} + \mathbf{P}$, so that the first two terms on the right side of expression (5) cancel. In general, instead of following directly behind the moving optimum, the phenotypic mean will trail to one side of the optimum (a flying-kite effect, see below) when there is strong correlational selection but no genetic correlation, or strong genetic correlation but no correlational selection. Thus, the shape of the adaptive landscape, in conjunction with the **G**-matrix, affects the degree to which the phenotypic mean lags behind the moving optimum, the direction of the lag, as well as the magnitude of directional selection that arises from that lag.

In a finite population, $\bar{\mathbf{z}}_t$, $\mathbf{G}$, and $\mathbf{P}$ will fluctuate. Starting with equation (4) and applying (3), while ignoring covariation between $\mathbf{G}_t$ and $\bar{\mathbf{z}}_t$ and variation of $\boldsymbol{\omega} + \mathbf{P}_t$ (which is likely to be appropriate because $\boldsymbol{\omega}$ is much larger than $\mathbf{P}_t$), we have instead of (5) the approximation

$$\mathrm{E}_t(\boldsymbol{\theta}_t - \bar{\mathbf{z}}_t) = (\boldsymbol{\omega} + \bar{\mathbf{P}})\bar{\mathbf{G}}^{-1}\boldsymbol{\Delta\theta}, \tag{6}$$

where E_t indicates expectation with respect to time, and $\bar{\mathbf{G}}$ and $\bar{\mathbf{P}}$ denote the expected values of $\mathbf{G}$ and $\mathbf{P}$ with respect to time.

Lande (1979) introduced the net (directional) selection gradient,

$$\boldsymbol{\beta}_T \equiv \sum_{t=0}^{T-1} \boldsymbol{\beta}_t = \bar{\mathbf{G}}^{-1}\Delta\bar{\mathbf{z}}_T, \tag{7}$$

as a retrospective measure of selection that is robust to change in the rate and direction of evolution. In (7), $\bar{\mathbf{G}}$ is the average **G**-matrix over the interval from generation 0 to generation $T - 1$, and $\Delta\bar{\mathbf{z}}_T = \bar{\mathbf{z}}_T - \bar{\mathbf{z}}_0$, the net change in the mean. For simplicity we will refer to $\boldsymbol{\beta}_T$ as net-$\boldsymbol{\beta}$. When $\Delta\bar{\mathbf{z}}_T$ represents the difference between the multivariate phenotypic means of two contemporary populations, this expression can be used to estimate the minimum amount of directional selection that is required to produce that differentiation (Lande 1979; Price et al. 1984; Schluter 1984; Price and Grant 1985; Lofsvold 1986; Arnold 1988; Pessoa and Reis 1991; Cheverud 1996).

Turelli (1988) argued that stochastic fluctuations in the **G**-matrix will lead to inaccuracy in estimating the net-$\boldsymbol{\beta}$ with the above expression. The source of inaccuracy is revealed in an expression that takes into account variation in $\mathbf{G}$

$$\boldsymbol{\beta}_T = \bar{\mathbf{G}}^{-1}\left[\Delta\bar{\mathbf{z}}_T - \sum_{t=0}^{T-1} (\mathbf{G}_t - \bar{\mathbf{G}})\boldsymbol{\beta}_t\right], \tag{8}$$

where $\mathbf{G}_t$ represents the **G**-matrix in generation t (Turelli 1988). The summation term on the right is proportional to the covariance between the **G**-matrix and the net selection gradient in the same generation. Turelli argued that large fluctuations in selection might cause this summation term to be relatively large even though fluctuations in $\mathbf{G}$ might be small. On the other hand, because selection in generation t will affect the **G**-matrix in generation $t + 1$, rather than in

generation t, one could argue that the summation term will be large only if there is autocorrelation in $\boldsymbol{\beta}_t$ (R. Lande, pers. comm.). One of our goals is to assess the size of Turelli's summation term and hence to evaluate the effect of stochastic variation in **G** on the estimation of net-$\boldsymbol{\beta}$.

Methods

The Simulation Model

The simulation-based model of multivariate evolution that we use in this study is a modification of the model used by Jones et al. (2003). These multivariate models are direct extensions of the univariate models employed by Bürger et al. (1989), Bürger and Lande (1994), and Bürger and Lynch (1995). In brief, we used a Monte Carlo approach to simulate a population of diploid, sexually reproducing organisms with two evolving quantitative traits. The life cycle consisted of: (1) production of progeny, including mutation and recombination; (2) viability selection; and (3) random selection of N adults from the survivors of selection. Viability selection was produced according to a Gaussian individual selection surface, such that the probability of survival of phenotype **z**, $W(\mathbf{z})$, was given by

$$W(\mathbf{z}) = \exp[-0.5(\mathbf{z} - \boldsymbol{\theta})^{\mathrm{T}}\boldsymbol{\omega}^{-1}(\mathbf{z} - \boldsymbol{\theta})]. \quad (9)$$

We imposed directional selection by changing the values of $\boldsymbol{\theta}$ at a constant rate over multiple generations of evolution. The mating system was monogamous and each breeding pair produced exactly four offspring. Under these circumstances, the effective population size is larger than the census population size. We used population sizes of 256, 512, 1024, and 2048, which corresponded to effective population sizes of 342, 683, 1366, and 2731 (Bürger and Lande 1994; Jones et al. 2003).

The two traits used in the simulations were determined by 50 pleiotropic, freely recombining, additive loci, which we modeled explicitly. Thus, the mutation of a particular allele changed its effects on both traits. These mutational effects were drawn randomly from a bivariate Gaussian distribution and added to the existing values of the allele, according to the continuum of alleles model (Crow and Kimura 1964). We focus on a Gaussian distribution of mutational effects, because the Gaussian distribution is the foundation of modern quantitative genetics. However, empirical evidence suggests that real mutations may not follow a Gaussian distribution, so other distributions of mutational effects warrant attention in future studies (Hill and Caballero 1992; Mackay et al. 1992). Nevertheless, we predict that our results will be robust to changes in the underlying distribution, given the small discrepancies in results produced by Gaussian and gamma distributions of mutational effects in the univariate case investigated by Bürger and Lande (1994). We used a distribution of mutational effects with means of zero, variances of α_1^2 and α_2^2, and a correlation of r_μ. This mutational correlation, r_μ, describes the extent to which the mutational effects are correlated. For example, when r_μ is positive, a mutation that increases an allele's effect on one trait will usually also increase its effect on the other trait. An individual's phenotype was determined by summing additive effects across loci and adding environmental variation, drawn from a Gaussian distribution with a mean of zero and a variance of one. For additional details on the basic model and its application to **G**-matrix stability under stabilizing selection, see Jones et al. (2003).

Our choice of parameter values starts with the parameters used in Jones et al. (2003) and Bürger and Lande (1994). In particular, we assume in the base model (i.e., unless otherwise noted) that each trait is determined by 50 unlinked pleiotropic loci, that the mutation rate (μ) is 0.0002 per haploid locus, that the variances of mutational effects (α_1^2 and α_2^2) are 0.05, and that the population size is 256 adults. Under most circumstances, the selection surface is rather shallow, with $\omega_{11} = \omega_{22} = 49$. We allow the mutational correlation (r_μ) to vary from 0.00 to 0.90 and the selectional correlation (r_ω) from -0.90 to 0.90.

The Moving Optimum

This study differs from the study described in Jones et al. (2003) in that we now allow the optimum to move, such that the population experiences directional selection in addition to the stabilizing selection modeled previously. The addition of a moving optimum adds several complications and parameters to the study. Clearly, the bivariate optimum might move in any direction and at any rate, so we confine our attention to a few interesting, representative cases. In one case the optimum of the first trait changes, while the other trait's optimum remains constant. This situation is most easily visualized as movement to the right (→) on a graph with the value of trait one on the x-axis and the value of trait two on the y-axis. We will also refer to this situation to movement of the optimum at an angle of 0°. In a second interesting case, both traits increase in value at the same rate, such that the optimum moves at a 45° angle (↗). In the third case that we explore in this study, the first trait increases in value while the second trait decreases in value at the same rate, and the optimum consequently moves along an angle of −45° (↘).

The rate at which the optimum moves is also an important consideration. In this study, we assume that the optimum moves at a constant rate, but that other features of the adaptive landscape (i.e., $\boldsymbol{\omega}$) remain constant. We have chosen a modest rate of movement under which the population can persist for long periods of time under any set of parameters that we investigate. The maximum rate of movement that we investigate is 0.01 units of environmental standard deviation per generation. For our most commonly used population size of 256, this rate of movement translates into approximately 0.008 haldanes or phenotypic standard deviations per generation. This rate is slightly faster than the geometric mean rate (0.0058) observed in a large sample of microevolutionary studies (Kinnison and Hendry 2001). When the optimum moves at angles of either 45° or −45°, we use magnitudes of per generation change for each trait of $0.01/(\sqrt{2})$, so that the geometric distance that the bivariate optimum moves is independent of the angle. We also performed a number of simulations with an optimum moving at a 10-fold slower rate. In those simulations the types of effects were qualitatively the same as in the simulations with a faster moving optimum but smaller in magnitude, so we do not present the results of those analyses.

We choose in the present study to use an optimum moving at a constant rate because it allows the population to achieve quasi-equilibrium between selection, drift, and mutation. From a genetically uniform starting population, we allow 10,000 generations for genetic variation to become established and equilibrate under stabilizing selection with a stationary optimum, followed by a period of 2000 generations of evolution under a moving optimum to allow for equilibration under that selection regime. These initial 2000 generations of selection under a moving optimum are followed by 2000 generations during which we tally genetic parameters each generation. These last 2000 generations are the experimental generations. Selection under an optimum moving at a constant rate is probably a more favorable scenario for **G**-matrix stability than short periods of intense directional selection followed by stabilizing selection (Turelli 1988). However, an optimum moving at a constant rate is more tractable from a modeling standpoint and consequently it is the first logical step in the exploration of changing selection regimes. The effects of periods of strong directional selection or an adaptive landscape with a changing shape would be worthy topics for future studies that build on the results that we present here.

*Measures of **G**-matrix Stability, Lag, Net-**β**, and the Turelli Effect*

During the evolution of the population and its **G**-matrix under a moving optimum, we tally numerous variables that relate to **G**-matrix stability, the lag of the population mean relative to the bivariate optimum, the actual and reconstructed values of net-**β**, and Turelli's summation term. The values of these various quantities provide insights into the stability of the **G**-matrix over evolutionary time and the reconstruction of the history of selection. First, we calculate the same values presented in the study of **G**-matrix stability by Jones et al. (2003). Every generation, we calculate the elements of the phenotypic variance-covariance matrix (P_{11}, P_{22}, P_{12}) and the **G**-matrix (G_{11}, G_{22}, G_{12}), the genetic correlation (r_g), and the eigenvalues of the **G**-matrix (λ_1 and λ_2). We also calculate the size (Σ), eccentricity (ϵ), and angle (φ) of the **G**-matrix (for definitions see Jones et al. 2003 or table footnotes). For all values presented in this paper, we calculate the mean across generations within an experimental run ($N = 2000$) and then present the means of these means across replicate runs ($N = 20$). Previous studies of this kind indicate that this approach seems to be appropriate on both empirical and theoretical grounds (Bürger et al. 1989; Bürger and Lande 1994; Jones et al. 2003). As an indication of **G**-matrix stability, we also calculate the single-generation changes in population variables (for additional details see Jones et al. 2003).

During the evolution of the simulated population, we can calculate both theoretical and realized lags relative to the optimum. Here, we represent the lags for the two traits as L_1 and L_2. The actual lag is simply the optimum minus the trait mean. We calculate these lags each generation and take the mean across generations to give the average lag for a particular run of the simulation. Values in the tables are means across 20 runs. The theoretical lag can be calculated according to equations (5) and (6). We calculate theoretical lags in two ways. First we calculate the theoretical lag each generation, using the corresponding **G**-matrix from that generation and then calculate the mean as we would do for the actual lag. In the second approach, we calculate the lag once at the end of each run, using the mean **G**-matrix for the entire simulation run.

One central goal of this study is to evaluate the impact of **G**-matrix stability or instability on the reconstruction of net-**β** in a retrospective analysis of selection. To accomplish this goal, we need to estimate **β** directly each generation. We use two approaches to estimate **β**. We use equation (4), and we use a multiple regression of relative fitness on trait values as outlined by Lande and Arnold (1983). Both techniques yield essentially identical estimates of **β,** so we use the more exact method given by equation (4) in our analyses. By calculating **β** each generation and summing across generations, we can obtain a direct estimate of net-**β** for each run of the simulation. We also obtain estimates of net-**β** from retrospective selection analysis based on equation (3), using **G** from four different sources. First, we use $\bar{\mathbf{G}}$, the average **G**-matrix over all experimental generations. Second, we use $\mathbf{G}_T$, the contemporary **G**-matrix. Third, we use the mean of the last two **G**-matrices, $\mathbf{G}_T$ and $\mathbf{G}_{(T-1)}$. Finally, we use the mean of the last five **G**-matrices, $\mathbf{G}_T$ through $\mathbf{G}_{(T-4)}$.

In the interest of understanding the complications arising during the retrospective analysis of selection, we also calculate Turelli's potentially confounding summation term (Turelli 1988; Shaw et al. 1995). This so-called Turelli effect, **τ**, is a column vector calculated according to equation (8). Rearranging equation (8) slightly, we define the Turelli effect as the summation term multiplied by the inverse of $\bar{\mathbf{G}}$, such that

$$\boldsymbol{\tau} = \bar{\mathbf{G}}^{-1} \sum_{t=0}^{T-1} (\mathbf{G}_t - \bar{\mathbf{G}})\boldsymbol{\beta}_t, \tag{10}$$

so that it is directly comparable in magnitude to the estimate of net-**β**. Thus, we can rewrite equation (8) as

$$\boldsymbol{\beta}_T = \bar{\mathbf{G}}^{-1} \Delta\bar{\mathbf{z}}_T - \boldsymbol{\tau}. \tag{11}$$

Clearly, the Turelli effect has the potential to cause inaccuracies in the estimation of net-**β**, and our intent was to investigate the expected magnitude of this term.

Results

We begin by presenting the results of the effects of peak movement on the stability properties of the **G**-matrix and comparing them with the main results of our previous study (Jones et al. 2003) of the effects of stabilizing selection toward a stationary optimum. Then we study the effects of peak movement on the size and shape of the **G**-matrix and on the evolution of the (bivariate) phenotypic mean. Finally, we explore the relationship between the net selection gradient (net-**β**) and the direction of peak movement as well as problems associated with the reconstruction of the net-**β** from data on the final generations of evolution.

G-Matrix Stability

In Jones et al. (2003), we showed that simple conditions for the stability properties of a (two-dimensional) **G**-matrix

TABLE 1. Average single-generation changes in the **G**-matrix under a moving optimum. The following parameters are fixed: $N_e = 342$, $\mu = 0.0002$ per locus per generation, $\alpha_1^2 = \alpha_2^2 = 0.05$, and $\omega_{11} = \omega_{22} = 49$. See the text for further details and definitions of symbols. The values of ΔG_{11}, ΔG_{22}, $\Delta\lambda_1$, $\Delta\lambda_2$, $\Delta\Sigma$, and $\Delta\epsilon$ have been standardized by dividing by their means (see Table 2 for means), whereas ΔG_{12}, Δr_g, and $\Delta\varphi$ are not standardized. Arrows indicate the direction of peak movement ($\Delta\boldsymbol{\theta}$), such that ↗ means that $\Delta\theta_1 = \Delta\theta_2 = 0.007071$, → means that $\Delta\theta_1 = 0.01$ and $\Delta\theta_2 = 0$, ↘ means that $\Delta\theta_1 = 0.007071$ and $\Delta\theta_2 = -0.007071$, and ● means that $\Delta\theta_1 = \Delta\theta_2 = 0$. Only means are shown in this table, but the standard deviations are typically much smaller than the means.

r_ω	r_μ	$\Delta\boldsymbol{\theta}$	ΔG_{11}	ΔG_{22}	ΔG_{12}	Δr_g	$\Delta\lambda_1$	$\Delta\lambda_2$	$\Delta\Sigma$	$\Delta\epsilon$	$\Delta\varphi$
0	0	●	0.072	0.072	0.023	0.050	0.071	0.072	0.05	0.10	9.67
0	0	↗	0.072	0.072	0.025	0.049	0.070	0.071	0.05	0.10	10.08
0	0	→	0.072	0.071	0.025	0.049	0.070	0.071	0.05	0.10	9.85
0	0	↘	0.072	0.072	0.026	0.049	0.070	0.071	0.05	0.10	9.92
0.75	0	●	0.073	0.073	0.018	0.047	0.071	0.073	0.05	0.10	6.54
0.75	0	↗	0.072	0.072	0.022	0.046	0.071	0.072	0.05	0.10	6.42
0.75	0	→	0.071	0.072	0.023	0.048	0.071	0.072	0.05	0.10	7.66
0.75	0	↘	0.073	0.072	0.023	0.049	0.071	0.072	0.05	0.10	9.55
0	0.5	●	0.073	0.073	0.023	0.040	0.072	0.071	0.06	0.10	3.32
0	0.5	↗	0.072	0.072	0.028	0.038	0.072	0.072	0.06	0.10	2.74
0	0.5	→	0.072	0.072	0.027	0.040	0.072	0.072	0.06	0.10	3.09
0	0.5	↘	0.072	0.072	0.026	0.040	0.072	0.071	0.06	0.10	3.40
0.75	0.5	●	0.072	0.072	0.023	0.035	0.072	0.073	0.06	0.10	2.32
0.75	0.5	↗	0.071	0.072	0.028	0.033	0.071	0.072	0.06	0.10	2.09
0.75	0.5	→	0.072	0.072	0.027	0.036	0.072	0.072	0.06	0.10	2.65
0.75	0.5	↘	0.071	0.072	0.029	0.037	0.071	0.072	0.06	0.10	2.65
0.9	0.9	●	0.073	0.073	0.030	0.010	0.073	0.071	0.07	0.10	0.70
0.9	0.9	↗	0.072	0.072	0.036	0.009	0.072	0.071	0.07	0.10	0.68
0.9	0.9	→	0.072	0.072	0.035	0.011	0.072	0.071	0.07	0.10	0.75
0.9	0.9	↘	0.071	0.072	0.036	0.011	0.072	0.071	0.07	0.10	0.74

can be established if it is described by its total size Σ, the shape parameter ϵ, and the orientation φ. Correspondingly, stability is measured by the average between generation changes $\Delta\Sigma$, $\Delta\epsilon$, and $\Delta\varphi$. The main results of that paper were that size and shape stability are promoted chiefly by large population size, whereas orientation stability is promoted by correlational selection, large population size, and especially by mutational correlation and the alignment of pleiotropic mutation and multivariate selection.

Table 1 presents results for a small subset of the parameter combinations for which we explored **G**-matrix stability. We examined three different conditions of peak movement, which are indicated by arrows in Table 1 (i.e., ↗, →, and ↘. The absolute rate of movement is the same in all three cases (see the legend of Table 1). We also present results from the stationary optimum (●) for comparison (Table 1). Examination of the data in Table 1 shows that peak movement has virtually no effect on the stability of quantities measuring the size of **G** (ΔG_{11}, ΔG_{22}, $\Delta\lambda_1$, $\Delta\lambda_2$, and $\Delta\Sigma$) or on the stability of its shape ($\Delta\epsilon$). There are, however, weak to moderate effects on the stability of the covariance and correlation (ΔG_{12} and Δr_g), and, in particular, on the orientation ($\Delta\varphi$). The strongest effects of peak movement on $\Delta\varphi$ (a decrease in stability) occur if $r_\omega = 0.75$ and $r_\mu = 0$, when movement is at $-45°$ (↘), which is perpendicular to the direction favored by correlational selection. Under these circumstances, the peak is moving across rather than along genetic lines of least resistance (Schluter 1996). If $r_\omega = 0$ and $r_\mu = 0.5$, then movement in the direction favored by mutational correlation (i.e., ↗, along genetic lines of least resistance) increases stability. These conclusions have been confirmed by many more parameter combinations (results not shown). Overall, our results indicate that the particular combination of r_ω and r_μ has (nearly) no effect on ΔG_{11}, ΔG_{22}, $\Delta\lambda_1$, $\Delta\lambda_2$, and $\Delta\epsilon$, but it does affect ΔG_{12}, Δr_g, $\Delta\Sigma$, and, very strongly, $\Delta\varphi$.

The effects of the interplay of selectional and mutational correlation on the stability of the orientation ($\Delta\varphi$) are documented in Figure 1. The three panels correspond to the three different directions of peak movement studied (↗, →, and ↘). Each panel displays the change in the orientation of the **G**-matrix as a function of the selectional correlation r_ω for five different values of r_μ. This figure clearly shows that independently of the direction of the peak movement, for positive mutational correlation the between-generation change of the angle, $\Delta\varphi$, always decreases with increasing selectional correlation unless the mutational correlation is very weak. In other words, mutational and selectional correlations of different signs lead to instability of the orientation. Without mutational correlation, an increase in selectional correlation, positive or negative, tends to increase stability of the orientation. However, this increase is much more pronounced if the optimum moves along lines of least genetic resistance (which is the direction of the leading eigenvalue of the selectional covariance matrix $\boldsymbol{\omega}$, i.e., the direction favored by correlational selection; Schluter 1996). By contrast, high positive (or negative) r_ω has almost no stabilizing effect if the optimum moves in the perpendicular direction. Of course, r_ω has little stabilizing effect when the angle is already stable due to high mutational correlation. Figure 1 also demonstrates that, as under pure stabilizing selection (see fig. 1 of Jones et al. 2003), mutational correlation is much more important in producing stability than correlational selection.

Figure 2 displays the effects on the stability of the orientation φ of the population size, unequal mutational variances, and unequal strength of stabilizing selection on the two traits. In each of the panels, the three different directions

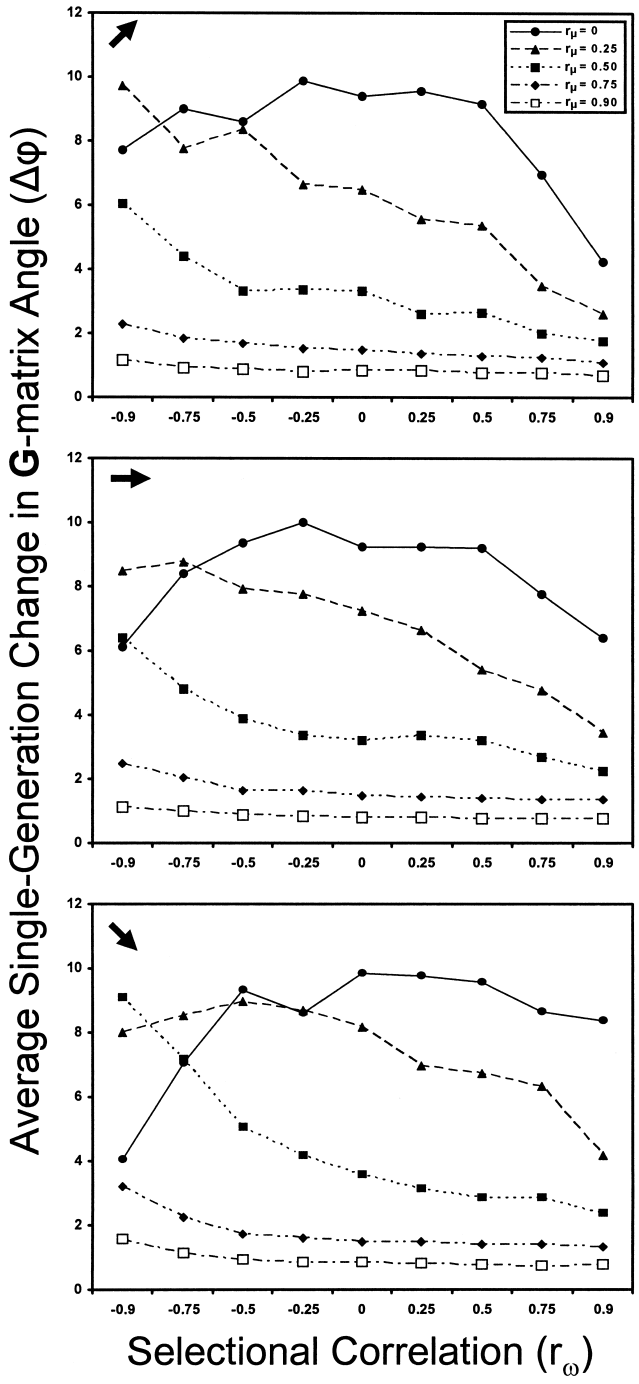

FIG. 1. The interplay of mutational and selection matrix alignment and direction of peak movement on stability of the angle (φ) of the **G**-matrix. This figure shows the average single-generation change in the **G**-matrix angle in a population of size $N_e = 342$, with various values of mutational and selectional correlations. Other parameters are the same as in Table 1. The top panel shows results for a bivariate optimum moving up and to the right (↗; both traits increasing), the middle panel shows results for an optimum moving to the right (→; trait one increasing, trait two stationary), and the bottom panel shows results for an optimum moving down to the right (↘; trait one increasing, trait two decreasing).

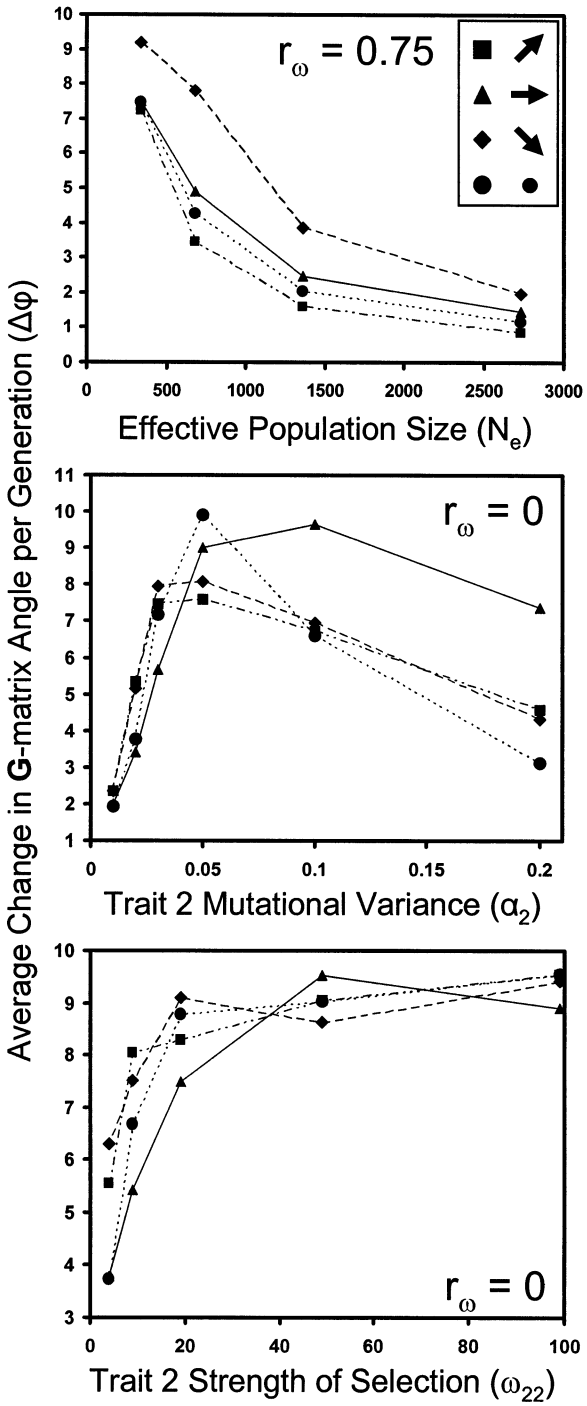

FIG. 2. The effects of population size, mutational variance, and unequal strengths of selection on the two traits on **G**-matrix stability. Different symbols represent different directions of peak movement as shown in the legend. The closed circles represent stabilizing selection only (no peak movement). In all cases, the mutational correlation (r_μ) is zero. All other parameters are the same as those used in Table 1, except as shown in the panels of this figure. The top panel shows the stabilizing influence of population size on the **G**-matrix. In the middle panel, the mutational variance for trait one (α_1^2) is held constant at 0.05, while the mutational variance for trait two (α_2^2) varies from 0.01 to 0.2. In the bottom panel, the strength of selection on trait one (ω_{11}) is held constant at 49, while the strength of selection on trait two (ω_{22}) is allowed to vary from four to 99.

of peak movement (↗, →, and ↘) are compared with the stationary optimum case. Most conspicuously, with a moving peak the stability properties of the orientation do not change qualitatively relative to a stationary one; however, there are quantitative effects. The upper panel demonstrates that increasing population size has a strong stabilizing effect on the orientation, and peak movement along the lines of least genetic resistance (in direction ↗ in this case) has a slight stabilizing effect relative to a stationary peak, whereas peak movement perpendicular to that direction (↘) has a distinctive destabilizing effect. The middle panel shows that unequal mutational variances (α_2^2 deviating from $\alpha_1^2 = 0.05$) have a strong stabilizing effect on φ. Trivially, in the absence of mutational variance (for one of the traits), any variation in φ vanishes. The third panel shows that increasing strength of stabilizing selection on the second trait always promotes stability of the orientation, the effect being most distinctive for a stationary optimum and an optimum moving only in direction of the first trait.

As for pure stabilizing selection, stability in size and shape are strongly enhanced by increasing population size, whereas other parameters have little effect (results not shown).

In summary, relative to a stationary optimum, a moving optimum has virtually no effects on the stability of the size Σ of the **G**-matrix nor on its shape ϵ, whereas it may stabilize or destabilize **G**-matrix orientation, φ. The stabilizing effect is most pronounced if the optimum moves along lines of least genetic resistance (e.g., the optimum moves in direction ↗ if r_ω is highly positive). Peak movement perpendicular to that direction has a destabilizing effect. Thus, the main conclusion of our previous study about **G**-matrix stability under stabilizing selection remain valid under directional selection caused by a moving optimum, nearly regardless of the direction and rate of movement; only a few new complimentary conditions have emerged. As for a stationary optimum, the most distinctive patterns are observed if the **G**-matrix is described by the parameters Σ, ϵ, and φ.

*Effects of Peak Movement on the Magnitude and Shape of **G***

Table 2 shows that peak movement always increases the size measures G_{11}, G_{22}, λ_1, λ_2, and Σ. This is in analogy to the univariate case (Bürger and Lynch 1995; Bürger 1999) and, presumably, caused by directional selection pushing favorable new alleles to fixation. During such selective sweeps, the genetic variance is substantially elevated, unless the population size is very small. We see this effect on both traits because pleiotropic mutations typically affect both traits, even in the absence of an average genetic correlation (for related phenomena arising in different models of pleiotropic selection, see Turelli 1985; Wagner 1989; Baatz and Wagner 1997). Also G_{12} sometimes increases, in particular if r_μ is not too small, although this does not necessarily translate into an elevated genetic correlation r_g. However, in the absence of mutational correlation, G_{12} may also be decreased if the optimum moves orthogonal to the direction favored by correlational selection ($r_\omega = 0.75$ and direction ↘). The genetic correlation r_g is little affected by peak movement, unless $r_\mu = 0$ and $r_\omega = 0.75$, when peak movement orthogonal to the direction favored by correlational selection leads to a substantial reduction. In general, the effects of peak movement on the shape parameter ϵ are very weak, except for a slight tendency of increasing ϵ (reducing eccentricity) if the direction of peak movement deviates from those favored by correlational mutation and/or selection. Also the orientation φ is nearly unchanged by peak movement except for the case $r_\mu = 0$ and $r_\omega = 0.75$. Then, φ decreases if the optimum moves in a direction deviating from that favored by correlational selection.

Effects of Peak Movement on the Phenotypic Mean

Peak movement induces directional selection on the population, causing the vector of phenotypic means, $\bar{\mathbf{z}} = (\bar{z}_1, \bar{z}_2)$, to evolve at the same rate as the optimum but lagging behind it. Eventually, unless mean fitness becomes so low that the population goes extinct (cf. Bürger and Lynch 1995), a kind of dynamical stationary state is attained in which the phenotypic mean deviates from the optimum by a constant average amount $\boldsymbol{\theta} - \bar{\mathbf{z}} = (\theta_1 - \bar{z}_1, \theta_2 - \bar{z}_2)^T = (L_1, L_2)^T$. Fluctuations about this mean occur because of random genetic drift and random mutations. Direction and amount of this lag depend on the direction and rate of peak movement, on the strength and correlation of the fitness landscape, and on the genetic properties of the population. Table 2 presents numerical data, and Figure 3 visualizes the most important effects. In all panels of Figure 3, the optimum moves in direction of the first trait and the second trait is under pure stabilizing selection (i.e., the direction of movement is →). The top panel shows that in the absence of selectional and mutational correlation, the mean of the first trait lags behind the optimum, whereas the mean of the second trait fluctuates randomly and without bias around $\theta_2 = 0$. Also orientation and shape of the **G**-matrix fluctuate substantially (for quantifications, see Table 1). The first and second panels of the figure show that, in the absence of mutational correlation, increasing correlational selection induces a systematic negative deviation of the mean of the second trait, $\bar{z}_2$, from its optimum $\theta_2 = 0$ (see Table 2, but note that a negative deviation from the optimum means a positive lag). The stabilizing effect on the orientation φ is also clearly visible (see Table 1). In contrast, in the absence of selectional correlation, increasing mutational correlation induces a large systematic positive deviation of $\bar{z}_2$ from its optimum $\theta_2 = 0$. Also the first traits develops a much larger lag, and a dramatic stabilization of the orientation and the shape of the **G**-matrix occurs (see Tables 1, 2 for quantifications). We call this the flying-kite effect. The stronger the mutational covariance, the higher the kite flies. However, as the bottom panel shows, strong correlational selection decreases the height at which the kite flies, possibly decreasing it to a small negative value. When the kite flies high, these large deviations of the mean phenotype $\bar{\mathbf{z}}$ from its optimum $\boldsymbol{\theta}$ induce such a large reduction in mean fitness that populations with relatively low reproductive potential become extinct.

Figure 4 shows the quantitative effects of increasing values of mutational and selectional correlations on the lag. As the selectional correlation increases, in the absence of mutational covariance, the lag of the first trait changes very little, whereas the lag of the second trait increases. As the mutational

TABLE 2. Mean values of population-level genetic variables. See Table 1 and the text for definitions of symbols and parameter values. This table presents means only. For each mean, we first calculated the mean across 2000 generations within each of 20 independent simulation runs. We then calculated the mean across these 20 independent means to obtain the means shown in this table. The actual lags of the phenotypic mean relative to the optimum are L_1 and L_2. $L_{1,\mathbf{G}(t)}$ and $L_{2,\mathbf{G}(t)}$ are the mean theoretical lags calculated each generation using the **G**-matrix for that generation, whereas $L_{1,\bar{\mathbf{G}}}$ and $L_{2,\bar{\mathbf{G}}}$, are theoretical lags calculated once at the end of each run using **G** (see text).

r_ω	r_μ	$\Delta\theta$	G_{11}	G_{22}	G_{12}	r_g	λ_1	λ_2	Σ^1	ϵ^2	φ^3	L_1	L_2	$L_{1,\mathbf{G}(t)}$	$L_{2,\mathbf{G}(t)}$	$L_{1,\bar{\mathbf{G}}}$	$L_{2,\bar{\mathbf{G}}}$
0	0	●	0.475	0.432	0.006	0.014	0.56	0.35	0.91	0.65	0.8	0.00	−0.02	0.00	0.00	0.00	0.00
0	0	↗	0.501	0.504	0.001	−0.001	0.61	0.39	1.00	0.65	−0.4	0.77	0.77	0.81	0.81	0.73	0.72
0	0	→	0.515	0.465	0.011	0.019	0.60	0.38	0.98	0.64	1.9	1.06	−0.03	1.12	−0.02	1.00	−0.02
0	0	↘	0.530	0.508	−0.022	−0.038	0.64	0.40	1.04	0.65	−8.1	0.72	−0.77	0.74	−0.76	0.66	−0.69
0.75	0	●	0.365	0.345	0.091	0.244	0.47	0.24	0.71	0.54	36.7	0.01	0.01	0.00	0.00	0.00	0.00
0.75	0	↗	0.417	0.434	0.104	0.234	0.56	0.29	0.85	0.55	37.8	1.32	1.31	1.33	1.32	1.20	1.19
0.75	0	→	0.469	0.419	0.074	0.159	0.57	0.32	0.89	0.59	25.0	1.09	0.69	1.10	0.70	0.99	0.63
0.75	0	↘	0.451	0.459	0.045	0.093	0.56	0.35	0.91	0.63	18.3	0.31	−0.22	0.29	−0.24	0.25	−0.22
0	0.5	●	0.424	0.423	0.181	0.430	0.62	0.23	0.85	0.38	44.4	−0.01	0.00	0.00	0.00	0.00	0.00
0	0.5	↗	0.500	0.480	0.242	0.488	0.74	0.24	0.98	0.34	43.7	0.52	0.55	0.53	0.57	0.49	0.51
0	0.5	→	0.516	0.465	0.218	0.443	0.73	0.26	0.98	0.37	41.2	1.34	−0.61	1.39	−0.66	1.24	−0.58
0	0.5	↘	0.481	0.484	0.207	0.423	0.70	0.26	0.96	0.39	45.0	1.42	−1.35	1.47	−1.45	1.32	−1.31
0.75	0.5	●	0.388	0.403	0.219	0.546	0.62	0.17	0.79	0.29	45.9	0.00	−0.01	0.00	0.00	0.00	0.00
0.75	0.5	↗	0.491	0.486	0.285	0.577	0.78	0.19	0.98	0.26	44.7	0.89	0.90	0.90	0.90	0.81	0.81
0.75	0.5	→	0.498	0.461	0.253	0.513	0.74	0.22	0.96	0.32	42.4	0.95	0.32	0.96	0.30	0.87	0.27
0.75	0.5	↘	0.508	0.505	0.263	0.499	0.78	0.23	1.01	0.33	45.5	0.43	−0.41	0.44	−0.43	0.40	−0.40
0.9	0.9	●	0.434	0.443	0.394	0.896	0.83	0.04	0.88	0.05	45.5	−0.02	−0.03	0.00	0.00	0.00	0.00
0.9	0.9	↗	0.526	0.529	0.478	0.903	1.01	0.05	1.05	0.05	45.1	0.72	0.73	0.76	0.76	0.69	0.68
0.9	0.9	→	0.517	0.503	0.454	0.886	0.97	0.05	1.02	0.06	44.6	1.06	−0.10	1.10	−0.11	0.98	−0.09
0.9	0.9	↘	0.530	0.528	0.472	0.887	1.00	0.06	1.06	0.06	44.9	0.78	−0.82	0.80	−0.86	0.73	−0.76

[1] We define the size, Σ, of the **G**-matrix as the sum of the eigenvalues.
[2] The eccentricity of the **G**-matrix, ϵ, is the smaller eigenvalue divided by the larger, so smaller values of ϵ reflect greater eccentricity.
[3] The angle of the **G**-matrix, φ, is simply the angle of the leading eigenvector, expressed as degrees with zero corresponding to the axis of the first trait.

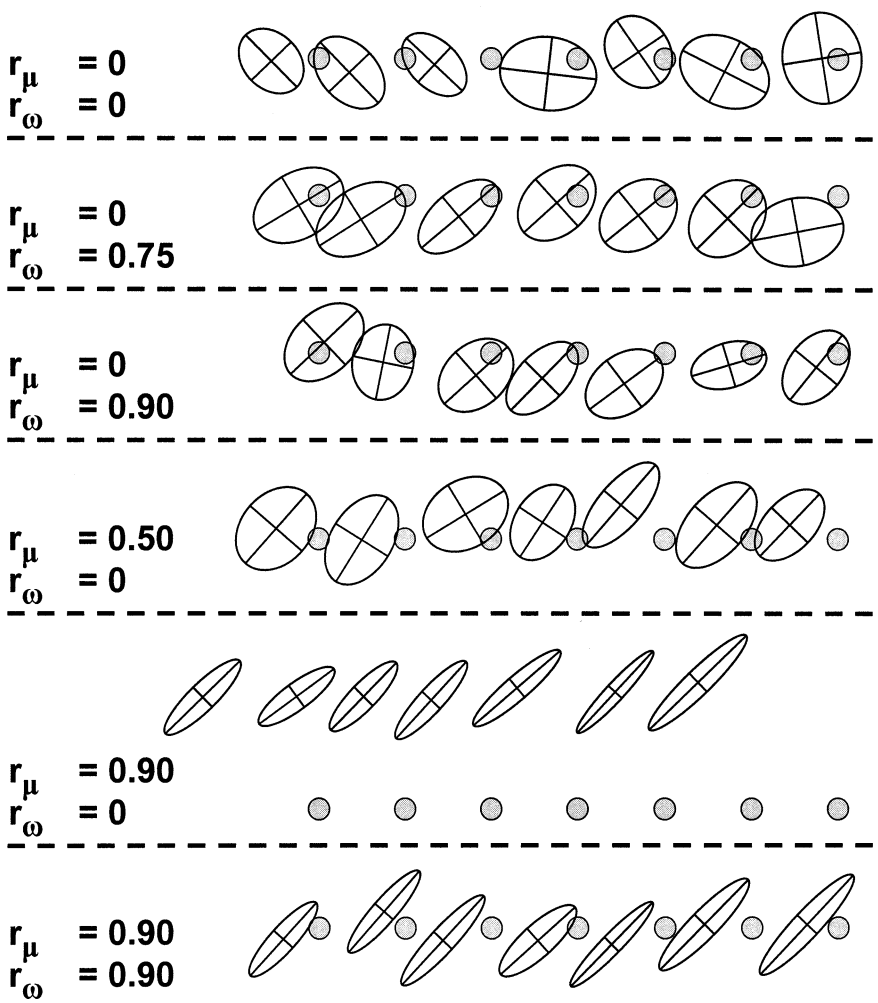

FIG. 3. Snapshots of the **G**-matrix and the position of the optimum for sample runs of the simulation. The bivariate optimum is represented by the small shaded circles. The **G**-matrix is represented as an ellipse, and the lines within the ellipse cross at the bivariate population mean. Each line has a length in each direction from the mean equal to 1.96 times the square root of the corresponding eigenvalue. Thus, these ellipses are expected to surround 95% of the breeding values in the population in any given generation. Note that these ellipses are drawn differently than those in Jones et al. (2003), in which the length along each axis was proportional to the corresponding eigenvalue rather than the square root of the eigenvalue. In this figure, the optimum of trait 1 is moving to the right and the optimum of trait 2 is not changing. The optimum and **G**-matrix are shown every 300 generations during simulation runs of 2100 generations. Parameter values are identical to those shown in Table 1, except that we also show an additional example with a very strong flying kite effect ($r_\omega = 0$, $r_\mu = 0.9$). Note that in this example (next to last panel), the population mean is lagging far to the left and above the position of the optimum.

correlation increases, in the absence of selectional correlation, the lag of the first trait increases, whereas the lag of the second trait decreases, thus demonstrating the flying kite effect. Figure 4 also shows the effects of effective population size (N_e) on the lag. The amount of lag, that is, the average length of the vector **L,** is a decreasing function of N_e (because the size of **G** increases with increasing N_e). Without presenting numerical results, our analyses also demonstrated that an increasing strength of stabilizing selection on the two traits decreases the lag, whereas a more rapidly moving optimum increases the lag.

Table 2 demonstrates further that the lag calculated from equation (5) by averaging over all generations provides a very accurate estimate of the real lag. Because equation (5) is based on the multivariate breeder's equation (eq. 3), this implies that, on average, (3) predicts the selection response of the mean very accurately. Even the estimate (6), which is based on numerically obtained $\bar{\mathbf{G}}$ and $\bar{\mathbf{P}}$, is surprisingly accurate although, in general, it slightly underestimates the absolute value of both components of the lag.

Reconstructing Net-$\boldsymbol{\beta}$

Reconstructions of historical selection patterns have relied on Lande's (1979) approximate expression (7) for the net selection gradient $\boldsymbol{\beta}_T$. This approximation requires constancy of the **G**-matrix. Table 3 as well as the upper row of graphs of Figure 5 show that, in general, the true net-$\boldsymbol{\beta}$ is very accurately predicted in our moving-optimum model by using equation (7), if $\bar{\mathbf{G}}$ is calculated from the simulations. However, closer inspection shows that (7) consistently underestimates the absolute values of both components of $\boldsymbol{\beta}_T$, the

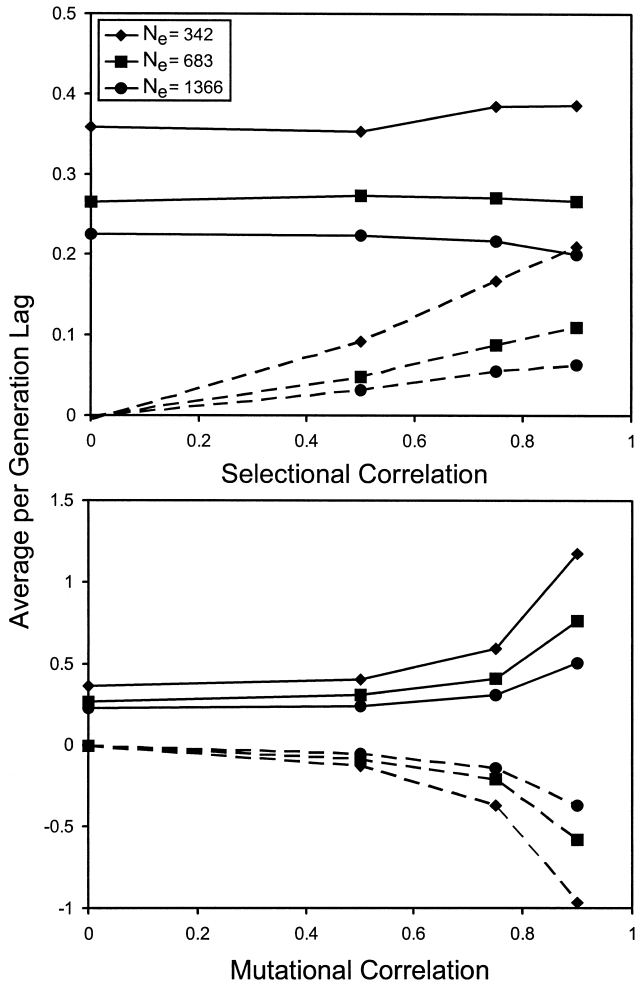

FIG. 4. Average lag of the phenotypic mean relative to the optimum for populations of different sizes and various values of mutational and selectional correlations. The parameters used to generate these graphs are the same as those used in Table 1, except that we use $\omega_{11} = \omega_{22} = 9$ and we perform the simulations using three different values of N_e. Different symbols correspond to effective population sizes of 342, 683, and 1366. The symbols connected by solid lines show results for trait 1; whereas those connected by broken lines show the results for trait 2. The top panel shows the effects of increasing correlational selection on the lag, and the bottom panel shows the effects of increasing mutational correlation on the lag.

error being on the order of about 10%. Moreover, Figure 5 shows that the R^2 from the regression of the estimated net-$\boldsymbol{\beta}$ on the true net-$\boldsymbol{\beta}$ is larger than 0.9. Thus, apart from the bias, equation (7) provides a very reliable estimate. This systematic bias can be explained by the Turelli effect. Turelli (1988) noted that if **G** is not constant, then (7) has to be replaced by (8), which is also based on the multivariate breeder's equation. Table 3 shows that this residual term indeed explains most of the bias. Should Turelli's (1988) article have caused despair among experimentalists (against the author's outspoken intention), then our investigation provides some comfort: the Turelli effect exists, but it is only on the order of about 5–10% of the main effect, at least under the circumstances we studied.

In practice, estimates of $\bar{\mathbf{G}}$ usually are not available, rather **G** is estimated from the last, or last few, generations. As shown by Table 3 and the lower row of graphs in Figure 5, on average estimates of net-$\boldsymbol{\beta}$ based on $\mathbf{G}_T$ instead of $\bar{\mathbf{G}}$ are very similar. However, as the regression analyses show (Figure 4), the R^2 value is much lower, implying that any single estimate based on $\mathbf{G}_T$ may be very inaccurate. Unfortunately, but, given the high serial autocorrelation in $\mathbf{G}_t$, not unexpectedly, estimation of net-$\boldsymbol{\beta}$ using the average over the last five generation of $\mathbf{G}_t$ does not increase R^2 (Fig. 6).

DISCUSSION

This study illustrates the effects of a moving optimum on the dynamics of the **G**-matrix in a finite population. Most of the important effects on **G**-matrix stability were captured by our previous study of **G**-matrix evolution under a static optimum (Jones et al. 2003), so nearly all of the conclusions of that study remain valid under a moving optimum as well. However, the addition of a moving optimum revealed additional complexities with respect to evolution of the **G**-matrix and the mean phenotype. This study is particularly important with respect to the dynamics of the mean phenotype and its lag relative to the optimum, the retrospective analyses of selection and the Turelli effect, and evolution along or across genetic lines of least resistance.

The Lag of the Phenotype and the Flying Kite Effect

Features of inheritance and selection that cause temporary maladaptation when the adaptive landscape is stationary can cause permanent departures from the peak when the peak is steadily moving. In the case of a stationary landscape, genetic correlation can deflect and substantially delay the approach of the phenotypic mean to the peak (Lande 1980b). The departures that we observed in our simulations were consistent with theoretical expectations. A dramatic example of departure is illustrated by the flying kite effect in which the phenotypic mean trails behind and above a moving optimum (Fig. 3). The largest departures are expected when the adaptive landscape and the **G**-matrix have opposing eigenvectors (i.e., anti-alignment in which the largest eigenvalue of one matrix corresponds to the smallest eigenvalue of the other matrix). In contrast, the flying kite effect is smallest when the eigenvectors of the two matrices are approximately aligned (e.g., $r_\omega = r_\mu$). In the alignment case, the contributions to lag by the **G**-matrix and the landscape cancel, see equation (5), so that the mean lags slightly behind the peak but not above or below it, except for fluctuations caused by drift or mutation (e.g., bottom panel in Fig. 3). The degree of lag (i.e., the length of vector $\mathbf{L} = \boldsymbol{\theta} - \bar{\mathbf{z}}$) is a decreasing function of Σ, the size of the **G**-matrix (Fig. 4).

Clearly, the lag of the mean has important implications for population persistence in changing environments (Lynch and Lande 1993; Bürger and Lynch 1995). As the population increasingly lags behind a moving peak, mean fitness decreases. If the decrease is large enough, the population can go extinct (Lynch and Lande 1993; Bürger and Lynch 1995). The decrease in mean fitness is expected to be a quadratic function of the lag of the population mean from its optimum (Lande 1980b). Because the lag itself is a function of the **G**-matrix, fluctuations in **G** will be amplified and may have

TABLE 3. Expected results of retrospective analysis of selection under different parameter combinations. See Table 1 for parameter values for these runs. The net $\boldsymbol{\Delta\theta}$ values show the total distance the optimum moved (in units of environmental standard deviations) over 2000 generations of evolution. The actual values of net-$\boldsymbol{\beta}$ were calculated by estimating $\boldsymbol{\beta}$ each generation according to equation (4) and summing across generations. Other columns show net-$\boldsymbol{\beta}$ calculated from retrospective selection analysis, using either the mean **G**-matrix (**G**) or the contemporary **G**-matrix ($\mathbf{G}_T$) for **G** in equation (3). The final two columns show the Turelli effect, $\boldsymbol{\tau}$, calculated from equation (10). All of the values in this table are means across 20 independent simulation runs.

				Actual values		Estimation from $\bar{G}$		Estimation from G_T		Turelli effect	
r_ω	r_μ	net $\Delta\theta_1$	net $\Delta\theta_2$	net-β_1	net-β_2	net-β_1	net-β_2	net-β_1	net-β_2	τ_1	τ_2
0	0	0.0	0.0	−0.2	−0.8	0.0	0.2	−0.1	0.2	0.1	0.2
0	0	14.1	14.1	30.7	30.3	29.0	28.5	30.8	29.3	−2.1	−2.0
0	0	20.0	0.0	42.2	−1.2	39.5	−0.5	43.2	−1.3	−3.1	0.3
0	0	14.1	−14.1	28.5	−30.3	26.5	−27.0	27.8	−30.3	−1.4	1.9
0.75	0	0.0	0.0	0.3	0.1	−0.1	0.4	−0.1	0.5	−0.2	0.1
0.75	0	14.1	14.1	31.4	29.0	28.4	27.1	30.5	27.4	−1.8	−1.5
0.75	0	20.0	0.0	50.1	−9.3	44.9	−7.0	51.7	−4.3	−3.0	0.8
0.75	0	14.1	−14.1	39.8	−37.6	35.4	−34.7	41.7	−36.5	−2.4	2.1
0	0.5	0.0	0.0	−0.5	0.0	−0.4	0.5	−0.2	0.5	0.5	−0.2
0	0.5	14.1	14.1	20.5	21.6	18.8	20.4	18.9	23.5	−1.4	−1.5
0	0.5	20.0	0.0	53.3	−24.4	49.4	−23.2	60.5	−30.8	−3.0	1.6
0	0.5	14.1	−14.1	56.3	−53.9	51.7	−51.7	58.2	−56.9	−3.1	2.2
0.75	0.5	0.0	0.0	0.7	−0.8	0.4	−0.4	0.4	−0.6	−0.1	0.1
0.75	0.5	14.1	14.1	19.7	21.3	18.4	18.8	21.6	20.9	−1.1	−1.2
0.75	0.5	20.0	0.0	61.6	−32.5	57.2	−31.1	70.5	−37.7	−3.7	1.5
0.75	0.5	14.1	−14.1	62.2	−61.8	58.5	−58.7	72.4	−72.7	−4.0	3.2
0.9	0.9	0.0	0.0	1.5	−2.4	−0.3	0.3	−0.7	0.7	0.5	−0.6
0.9	0.9	14.1	14.1	14.3	16.3	14.7	13.8	19.5	13.6	−1.0	−0.8
0.9	0.9	20.0	0.0	205.6	−185.5	188.2	−169.8	191.1	−167.3	−12.0	10.9
0.9	0.9	14.1	−14.1	267.4	−268.1	250.3	−251.2	254.1	−252.5	−10.7	10.7

large negative effects on mean fitness. Thus, even when the population is potentially able to keep up with a moving peak (i.e., maintain a constant lag), stochastic fluctuation in **G** and hence in mean fitness may drive it extinct. Conditions that stabilize the **G**-matrix under a selection regime with a moving optimum are also conditions that favor population persistence.

The Maintenance of Genetic Variance under a Moving Optimum

Peak movement can increase genetic variation and covariation relative to a static peak. In other words, the addition of directional selection increases the genetic variance relative to stabilizing selection alone. This effect on genetic variance has been found in past simulations of directional selection (Bürger and Lynch 1995; Bürger 1999). The increase in genetic variances apparently arises because the directional selection induced by peak movement causes a recurrent pattern of favorable alleles sweeping toward fixation (Barton and Turelli 1987). Each selective sweep boosts genetic variance. Even when peak movement changes the optimum of only one trait, pleiotropy of alleles sweeping toward fixation increases the genetic variance of the other trait as well as the genetic covariance between the two traits. In large populations the increase in genetic variance due to peak movement can be considerable (Bürger and Lynch 1995; Bürger 2000). For example, in our simulations involving effective population sizes of 2731 individuals, the largest increase in the genetic variance for trait one occurred when the optimum moved to the right. Regardless of the values of the mutational and selectional correlations, a population evolving in response to an optimum moving to the right maintained approximately 150–200% of the genetic variance present in a population experiencing stabilizing selection alone.

The Stability of G under a Moving Optimum

Promotion of **G**-matrix stability by peak movement was an unanticipated result. Although peak movement has virtually no effect on the stability of eigenvalues (as registered in **G**-matrix size and eccentricity), it can have a small stabilizing effect on the angle of the **G**-matrix. In particular, the stabilizing effect arises when peak movement reinforces the evolution of a cigar-shaped **G**-matrix. Thus, alignment of the mutation matrix and the adaptive landscape (e.g., $r_\mu = r_\omega = 0.9$) produces a cigar-shaped **G**-matrix (Fig. 3, bottom panel). When the peak moves along the long axis of the cigar (the genetic line of least resistance; Schluter 1996), the angle of the **G**-matrix becomes especially stable (Table 1; Figs. 1, 2).

In contrast, the **G**-matrix tends to be less stable when the optimum moves across genetic lines of least resistance. A stationary optimum (i.e., stabilizing selection only) generally produces a **G**-matrix that is intermediate in stability relative to either a peak moving along or across genetic lines of least resistance. Thus, in addition to alignment of the mutational and selectional correlations, alignment of the direction of peak movement with these correlations also enhances **G**-matrix stability, at least with respect to orientation. In some cases this effect is very pronounced. For example, when the mutational correlation is very weak, but the selectional cor-

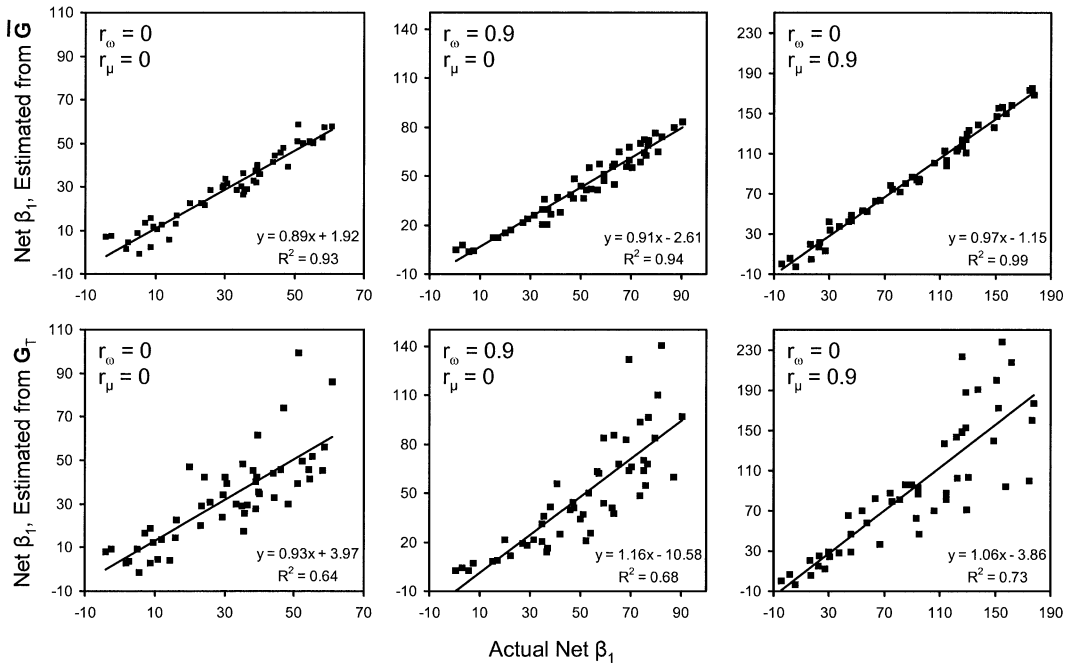

FIG. 5. Estimation of net-**β** from retrospective selection analyses. For these graphs, we allow the optimum for trait 1 to increase, while the optimum of trait 2 is held constant. The *x*-axis shows the actual net-**β** calculated directly each generation and summed across the 2000 generations. The *y*-axis shows the results of retrospective selection analysis, using either the mean **G**-matrix (averaged across all 2000 generations) or the contemporary **G**-matrix (from the last generation) in equation (3). Each point in the graph represents the results from a single run of the simulation (i.e., analogous to what one would have in a real empirical assessment of selection). We introduce variation in **β** by allowing the first trait's optimum to move at different rates during the different runs. In the four leftmost panels, $\Delta\theta_1$ ranged from 0.00 to 0.05 in intervals of 0.001. In the two rightmost panels, $\Delta\theta_1$ ranged from 0.00 to 0.02 in intervals of 0.0004. Note that within a run $\Delta\theta_1$ is constant (and this is true for the entire study), but each of the points on a given graph was generated using runs with different values of $\Delta\theta_1$. This approach was necessary to generate variance in the actual value of **β.**

relation is strongly positive, movement of the optimum across genetic lines of least resistance essential cancels out any benefit in stability gained by the high correlational selection (Fig. 1, rightmost filled circle, compared among the three panels).

Our simulations neglect some potentially important influences on **G**-matrix stability. First, although peak movement with constant direction and speed may characterize some selection regimes in nature (e.g., global warming), peak movement may be variable in speed and direction under many other circumstances (Arnold et al. 2001). In such cases of temporal variation in the rate and direction of peak movement, the angle of the **G**-matrix is probably less stable than in the cases examined in the present report, although size and eccentricity stability are not likely to be affected. Second, change in the shape (curvature) of the adaptive landscape is conceivable in some circumstances. Relaxation of selection pressures (e.g., due to decreased competition) could correspond to increased width of the adaptive landscape. If relaxation did not change the orientation of the landscape, so that the eigenvectors of **ω** + **P** remained unchanged, then the average orientation of the **G**-matrix would not be affected, although its angle would be less stable. Third, change in the orientation of the landscape could affect both the average angle of the **G**-matrix and its stability. Trait evolution that alters functional connections among characters (i.e., changes correlational selection) could have this kind of effect. Fourth, the pattern of pleiotropic mutation remains constant in our simulations. It seems likely that the mutation matrix itself evolves in response to directional and stabilizing selection. Thus, features of the environment and trait interaction that impart instability to the mutation matrix will also promote instability of the **G**-matrix. We hope to address some of these influences on **G**-matrix stability in future reports.

Retrospective Analysis of Selection

Our results are encouraging for empiricists in that they indicate that the true net-**β** can be accurately reconstructed under some circumstances. In particular, using Lande's (1979) expression, we were able to accurately estimate the magnitude of net-**β** when we used a value of **G** based on the entire sequence of 2000 generations. Although the estimation was relatively accurate in this case, there was a small systematic bias such that net-**β** was consistently underestimated. This bias increased linearly with true net-**β** (Figure 5), and was almost certainly a consequence of the Turelli effect (Turelli 1988; Shaw et al. 1995).

Even though the Turelli effect introduced a systematic bias in the estimation of net-**β,** the magnitude of this bias was generally small in our simulations. This effect, which arises due to within-generation covariance between **G** and **β,** was typically about 5–7% of net-**β** when the effective population size was 342. Interestingly, as the population size increases, the relative magnitude of the Turelli effect decreases, such that in our largest populations, with N_e = 2731, the Turelli effect was only about 1–2% the magnitude of net-**β**. Although

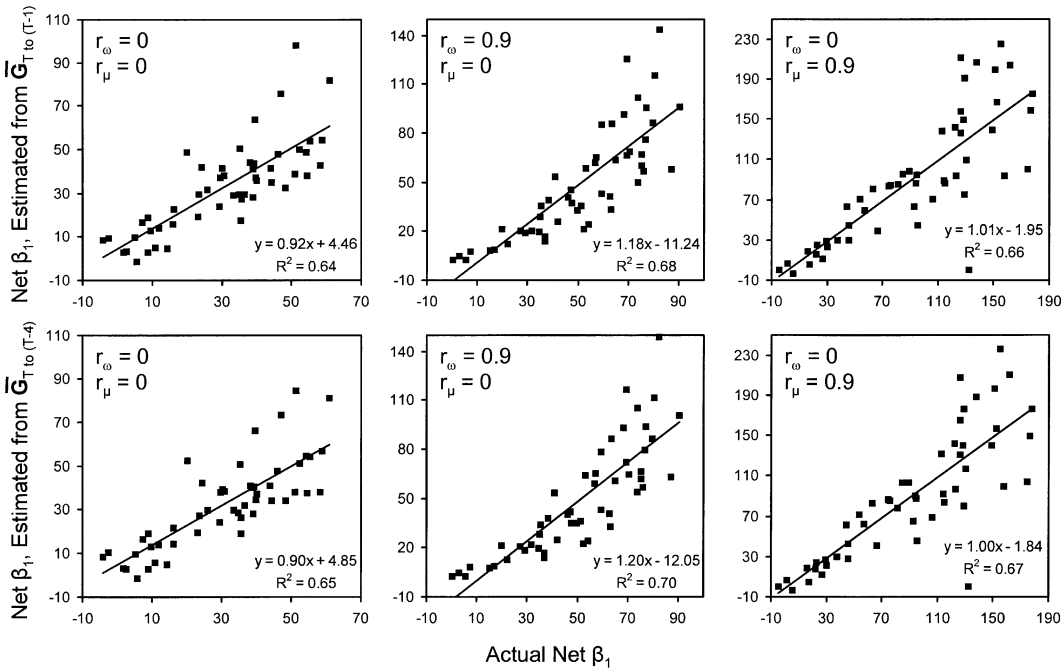

FIG. 6. Reconstruction of net-**β** from the last two or five **G**-matrices from the population. These graphs are the same as those shown in Figure 5, except that the retrospective selection analysis uses either the mean of **G**-matrices from the last two (top) or five (bottom) generations of evolution. This situation is analogous to an empirical attempt to obtain a better estimate of the **G**-matrix by calculating genetic parameters from several recent generations of the population under study.

a Turelli effect of this magnitude might be considered a tolerable source of error in a calculation using real data, under some circumstances the effect could be considerably larger. The consistently negative sign of the summation term indicates that the covariance between **G** and **β** was negative in our simulations. The effect of this negative sign would be a consistent tendency to underestimate net-**β** using Lande's (1979) expression. In particular, this underestimation could occur if large deviations in **β** happen in episodes consisting of at least a few generations in a row, so that deviations in **β** are positively autocorrelated. Such a temporal pattern could lead to the accumulation of within-generation covariance between **G** and **β**. Thus, it clearly is possible to concoct scenarios under which the Turelli effect is a serious problem for retrospective selection analyses. However, the general message of our results is that under many circumstances it may not seriously complicate estimation of net-**β,** particularly in analyses involving large populations.

One important caveat regarding our interpretation of the importance of the Turelli effect is that we did not investigate selection of the type that Turelli (1988) believed would be most likely to produce covariance between **G** and **β**. Turelli believed that large fluctuations in the intensity and direction of selection would be most likely to produce a correlation between **G** and **β**. In our study, we used a constant rate of peak movement, resulting in fairly small fluctuations in the intensity of selection. Fluctuating selection is beyond the scope of the current study, so it remains to be seen whether the Turelli effect is more important under such circumstances.

Accuracy in estimation of net-**β** from real data will depend on how well $\bar{\mathbf{G}}$ is estimated. Our simulations indicate that the use of a single **G**-matrix to estimate $\bar{\mathbf{G}}$ could lead to a highly erroneous estimate for the magnitude of net-**β**. Some of the outliers in Figure 5 represent large overestimates of net-**β.** Unfortunately, the prospects for reconstructing net-**β** do not improve considerably when multiple recent generations are used to estimate **G** (Fig. 6). With up to the five most recent generations used to estimate $\bar{\mathbf{G}}$, the reconstruction of net-**β** still does not improve appreciably. Thus, our results strongly suggest that it is not a useful exercise to estimate the **G**-matrix from multiple generations within a population in hopes of improving the accuracy of retrospective selection analyses. This phenomenon is a consequence of the high autocorrelation of $\bar{\mathbf{G}}$ (Jones et al. 2003). In reality, the prospects for estimating **G** from contemporary populations may be even worse than the impression given by our analysis, because in the simulations we know the exact **G**-matrix each generation. In empirical studies of real organisms, error in the estimation of $\bar{\mathbf{G}}$ will further hinder the pursuit of an accurate estimate of $\bar{\mathbf{G}}$. The only hope for good estimates of $\bar{\mathbf{G}}$ probably will come from comparative studies of **G** in a phylogenetic context.

One other interesting result regarding the reconstruction of patterns of selection is that a more stable **G**-matrix has only a modest effect on the accuracy of estimation of net-**β.** For example, a mutational correlation of 0.90 produces a **G**-matrix with extremely stable orientation (Fig. 3), and yet almost as much error surrounds the estimation of net-**β** in a population with this high mutational correlation as in a population with no mutational or selectional correlations (Fig. 5). This phenomenon is partially due to the fact that correct estimation of net-**β** depends not only on the orientation of the **G**-matrix, but also on the size of **G.** It may also be caused partially by the fact that unstable **G**-matrices tend to be round

and do not seriously constrain the path of evolution, whereas stable **G**-matrices do constrain the path but the constraints are better estimated due to their high stability.

Our results help clarify the different inferences that can be made from net-**β** and from a net change in the phenotypic mean. Net-**β** describes the minimum force of directional selection required to account for an observed change in the mean, assuming that selection acts through a particular or average **G**-matrix (Lande 1979). Although a moving adaptive peak will induce directional selection, net-**β** does not provide a reconstruction of peak movement. Once a population has reached quasi-equilibrium between directional selection, drift, and mutation, however, the lag of the multivariate phenotype will remain relatively constant and the net change in the phenotypic mean will approximately equal net peak movement. In contrast, net-**β** will often give an inaccurate picture of peak movement, especially when genetic correlation is high and the optimum phenotype of only one character changes (Table 3). For example in the penultimate panel of Figure 3, there is persistent directional selection on trait two, even though its optimum never deviates from zero.

*Empirical Observations of **G**-Matrix Stability*

One of the most interesting results from comparative studies of **G**-matrices is the observation that eigenvectors can be conserved even when eigenvalues vary (Arnold 1981; Arnold and Phillips 1999; Roff and Mousseau 1999). The observation of conserved eigenvectors is especially notable because it is seen between sister populations with divergence times ranging from tens of generations to hundreds of thousands of generations. What do our simulation results tell us about this kind of stability? In our simulations, conservation of eigenvectors is revealed as small per generation change in the angle of the leading eigenvector of the **G**-matrix (i.e., by small average $\Delta\varphi$). In our simulations we held the multivariate patterns of mutation and selection constant. We found that conservation of eigenvectors (orientation stability) was promoted by large population size, pleiotropic mutation (mutational covariance), correlational selection, alignment of mutation and selection, steady movement of the selective optimum, and alignment of that movement with mutation and selection. Leaving aside population size and mutation for the moment, all of these orientation-stabilizing factors can be visualized in terms of a particular kind of adaptive landscape. That landscape has an evolutionarily persistent shape that consists of a cigar-shaped hilltop oriented at some angle to the trait axes, so that it produces strong correlational selection. The main axis of the hill is aligned with the evolutionarily persistent axis of the matrix that describes mutational variation. These circumstances are sufficient to produce a **G**-matrix that is in alignment with both mutation and selection. Finally, the hilltop moves in a direction that is in alignment with mutation, selection, and the **G**-matrix. The direction of movement corresponds to the genetic line of least resistance (Schluter 1996), but it also corresponds to the leading eigenvalue of the adaptive landscape, which Arnold et al. (2001) called the ''selective line of least resistance.'' Although this particular vision of an adaptive landscape with a moving optimum is the one most conducive to orientation stability of the **G**-matrix, all of these factors and their several alignments may not have played a role in the observed instances of **G**-matrices with conserved eigenvectors. Nevertheless, it seems inevitable that some subset of these factors is responsible for the observed conservation of orientation. The tasks before us are to determine whether conservation of **G** orientation is sufficiently common to warrant our continued attention and, if so, to devise tests that identify which candidate factors are responsible for that conservation.

Conclusions

Our simulation-based model of the dynamics of the **G**-matrix under persistent directional selection advances our understanding of several important issues in quantitative genetics. First, most major influences on **G**-matrix stability can be illustrated in the stabilizing selection case explored by Jones et al. (2003). The only major surprise with respect to **G**-matrix stability under a moving optimum is that movement along genetic lines of least resistance enhances stability of the orientation of the **G**-matrix, whereas movement across these lines decreases stability. Our second major result is that a persistently moving adaptive landscape can produce chronic maladaptation through the flying kite effect, even at traits whose optima are not changing. This effect is most pronounced when the **G**-matrix is stable, providing another phenomenon for which **G**-matrix stability is important. Another important point, which is not new to our study but also is not widely appreciated, is that a trait experiencing directional selection due to a moving optimum will exhibit greater genetic variance than the same trait experiencing only stabilizing selection. Finally, we gained several new insights into the reconstruction of the history of selection through the estimation of net-**β.** The Turelli effect is certainly real, caused by negative covariance between **β** and **G**, but its magnitude relative to net-**β** is small, suggesting that it may not seriously complicate retrospective selection analysis, at least for a population experiencing a persistently moving optimum. We also found that the average **G**-matrix, $\bar{\mathbf{G}}$, produced a very good estimate of net-**β,** whereas estimates based on only the contemporary **G**-matrix were prone to error. Averaging over a few recent generations did not help appreciably, so the best approach to the estimation $\bar{\mathbf{G}}$ is probably to infer it from comparative analysis involving closely related species or populations.

Acknowledgments

We thank P. C. Phillips and the **G**-matrix seminar group at the University of Oregon and Oregon State University for helpful discussion. This work was supported by funds from the National Institutes of Health (AGJ), the National Science Foundation (SJA), and Georgia Institute of Technology (AGJ).

Literature Cited

Arnold, S. J. 1981. Behavioral variation in natural populations. I. Phenotypic, genetic, and environmental correlations between chemoreceptive responses to prey in the garter snake, *Thamnophis elegans*. Evolution 35:489–509.

———. 1988. Quantitative genetics and selection in natural pop-

ulations: microevolution of vertebral numbers in the garter snake *Thamnophis elegans*. Pp. 619–636 *in* B. S. Weir, E. J. Eisen, M. M. Goodman, and G. Namkoong, eds. Proceedings of the 2nd international conference on quantitative genetics. Sinauer, Sunderland, MA.

Arnold, S. J., and P. C. Phillips. 1999. Hierarchical comparison of genetic variance-covariance matrices. II. Coastal-inland divergence in the garter snake, *Thamnophis elegans*. Evolution 53: 1516–1527.

Arnold, S. J., M. E. Pfrender, and A. G. Jones. 2001. The adaptive landscape as a conceptual bridge between micro- and macroevolution. Genetica 112/113:9–32.

Baatz, M., and G. P. Wagner. 1997. Adaptive inertia caused by hidden pleiotropic effects. Theor. Popul. Biol. 51:49–66.

Barton, N. H., and M. Turelli. 1987. Adaptive landscapes, genetic distance and the evolution of quantitative characters. Genet. Res. 49:157–173.

Bürger, R. 1999. Evolution of genetic variability and the advantage of sex and recombination in changing environments. Genetics 153:1055–1069.

———. 2000. The mathematical theory of selection, recombination, and mutation. John Wiley and Sons, Chichester, U.K.

Bürger, R., and R. Lande. 1994. On the distribution of the mean and variance of a quantitative trait under mutation-selection-drift balance. Genetics 138:901–912.

Bürger, R., and M. Lynch. 1995. Evolution and extinction in a changing environment: a quantitative genetic analysis. Evolution 49:151–163.

Bürger, R., G. P. Wagner, and F. Stettinger. 1989. How much heritable variation can be maintained in finite populations by mutation-selection balance? Evolution 43:1748–1766.

Charlesworth, B., R. Lande, and M. Slatkin. 1982. A neo-Darwinian commentary on macroevolution. Evolution 36:474–498.

Cheverud, J. M. 1996. Quantitative genetic analysis of cranial morphology in the cotton-top (*Saguinus oedipus*) and saddle-back (*S. fuscicollis*) tamarins. J. Evol. Biol. 9:5–42.

Crow, J. F., and M. Kimura. 1964. The theory of genetic loads. Pp. 495–505 *in* S. J. Geerts, ed. Proceedings of the 11th international congress of genetics. Pergamon, Oxford, U.K.

Hill, W. G., and A. Caballero. 1992. Artificial selection experiments. Annu. Rev. Ecol. Syst. 23:287–310.

Jones, A. G., S. J. Arnold, and R. Bürger. 2003. Stability of the **G**-matrix in a population experiencing pleiotropic mutation, stabilizing selection, and genetic drift. Evolution 57:1747–1760.

Kingsolver, J. G., H. E. Hoekstra, J. M. Hoekstra, D. Berrigan, S. N. Vignieri, C. E. Hill, A. Hoang, P. Gilbert, and P. Beerli. 2001. The strength of phenotypic selection in natural populations. Am. Nat. 157:245–261.

Kinnison, M. T., and A. P. Hendry. 2001. The pace of modern life. II. From rates of contemporary microevolution to pattern and process. Genetica 112/113:145–164.

Kohn, L. A. P., and W. R. Atchley. 1988. How similar are genetic correlation structures? Data from mice and rats. Evolution 42: 467–481.

Lande, R. 1979. Quantitative genetic analysis of multivariate evolution applied to brain:body size allometry. Evolution 33: 402–416.

———. 1980a. The genetic covariance between characters maintained by pleiotropic mutations. Genetics 94:203–215.

———. 1980b. Genetic variation and phenotypic evolution during allopatric speciation. Am. Nat. 116:463–479.

Lande, R., and S. J. Arnold. 1983. The measurement of selection on correlated characters. Evolution 37:1210–1226.

Lofsvold, D. 1986. Quantitative genetics of morphological differentiation in *Peromyscus*. I. Tests of the homogeneity of genetic covariance structure among species and subspecies. Evolution 40:559–573.

Lynch, M. 1989. The distribution of life history variation in *Daphnia pulex*. Evolution 43:1724–1736.

Lynch, M., and R. Lande. 1993. Evolution and extinction in response to environmental change. Pp. 234–250 *in* P. Kareiva, J. Kingsolver, and R. Huey, eds. Biotic interactions and global change. Sinauer Associates, Sunderland, MA.

Lynch, M., W. Gabriel, and A. M. Wood. 1991. The adaptive and demographic response of plankton populations to environmental change. Limnol. Oceanogr. 36:1301–1312.

Mackay, T. F. C., R. F. Lyman, and M. S. Jackson. 1992. Effects of P elements on quantitative traits in *Drosophila melanogaster*. Genetics 130:315–332.

Paulsen, S. M. 1996. Quantitative genetics of the wing color pattern in the buckeye butterfly (*Precis coenia* and *Precis evarete*): evidence against the constancy of **G**. Evolution 50:1585–1597.

Pessoa, L. M., and S. F. D. Reis. 1991. Natural selection, morphological divergence, and phenotype evolution in *Prechimys dimidiatus*: Rodentia, Echimyidae. Rev. Bras. Genet. 14:705–712.

Phillips, P. C., M. C. Whitlock, and K. Fowler. 2001. Inbreeding changes the shape of the genetic covariance matrix in *Drosophila melanogaster*. Genetics 158:1137–1145.

Price, T. D., and P. R. Grant. 1985. The evolution of ontogeny in Darwin's finches: a quantitative genetic approach. Am. Nat. 125: 169–188.

Price, T. D., P. R. Grant, and P. T. Boag. 1984. Genetic changes in the morphological differentiation of Darwin's ground finches. Pp. 49–66 *in* K. Wohrmann and V. Loeschcke, eds. Population biology and evolution. Springer-Verlag, Berlin.

Reeve, J. P. 2000. Predicting long-term response to selection. Genet. Res. 75:83–94.

Roff, D. A., and T. A. Mousseau. 1999. Does natural selection alter genetic architecture? An evaluation of quantitative genetic variation among populations of *Allonemobius socius* and *A. fasciatus*. J. Evol. Biol. 12:361–369.

Schluter, D. 1984. Morphological and phylogenetic relations among the Darwin's finches. Evolution 38:921–930.

———. 1996. Adaptive radiation along genetic lines of least resistance. Evolution 50:1766–1774.

Schmalhausen, I. I. 1949. Factors of evolution, the theory of stabilizing selection. Univ. of Chicago Press, Chicago.

Shaw, F. H., R. G. Shaw, G. S. Wilkinson, and M. Turelli. 1995. Changes in genetic variances and covariances: **G** whiz! Evolution 49:1260–1267.

Simpson, G. G. 1944. Tempo and mode in evolution. Columbia Univ. Press, New York.

———. 1953. The major features of evolution. Columbia Univ. Press, New York.

Steppan, S. J., P. C. Phillips, and D. Houle. 2002. Comparative quantitative genetics: evolution of the **G** matrix. Trends Ecol. Evol. 17:320–327.

Turelli, M. 1985. Effects of pleiotropy on predictions concerning mutation-selection balance for polygenic traits. Genetics 111: 165–195.

———. 1988. Phenotypic evolution, constant covariances, and the maintenance of additive variance. Evolution 42:1085–1089.

Turelli, M., and N. H. Barton. 1990. Dynamics of polygenic characters under selection. Theor. Popul. Biol. 38:1–57.

Wagner, G. P. 1989. Multivariate mutation-selection balance with constrained pleiotropic effects. Genetics 122:223–234.

Wagner, G. P., G. Booth, and H. Bagheri-Chaichian. 1997. A population genetic theory of canalization. Evolution 51:329–347.

Wilkinson, G. S., K. Fowler, and L. Partridge. 1990. Resistance of genetic correlation structure to directional selection in *Drosophila melanogaster*. Evolution 44:1990–2003.

Corresponding Editor: J. Fry